

# EXPERIMENTAL REPRODUCTION OF BRAIDED CHANNELS AND BEDFORMS WITH THREE DIFFERENT SCALES OBSERVED IN MOUNTAIN RIVERS

By

H. Meguro

National Institute for Land and Infrastructure Management, Tsukuba, Japan

K. Hasegawa

Professor

Graduate school of Engineering, Hokkaido University, Sapporo, Japan

and

K. Nakamura

Graduate student of Doctor Degree,

Graduate school of Engineering, Hokkaido University, Sapporo, Japan

## SYNOPSIS

The bedforms of Mountain Rivers have three different scales: large-, medium- and small- scales. The origins and properties of two kinds of small-scale bedforms and one kind of medium-scale bedform have become evident, but little is known about the origins and properties of large-scale bedforms. In this study, experiments using a steep slope flume with a movable bed composed of heterogeneous materials were conducted for in order to reproduce large-scale bedforms and bedforms of three different scales. In these experiments, bedforms of three different scales, which are very similar to those in natural Mountain Rivers, were reproduced in the flume. Findings reveal that one of the origins of large-scale bedforms is related to multi-row bars formed by large floods which fill up the valley width.

## INTRODUCTION

There are three different scales of bedforms in Mountain Rivers: a small-scale bedforms, which are known as step and pool systems, whose wavelengths are severalfold water depth; medium-scale bedforms, which are alternating bars, and whose wavelengths are severalfold river width; and large-scale bedforms, whose wavelengths are severalfold valley width (4)(5)(6). The origins and hydraulic properties of these bedforms have become evident in recent studies. Studies have shown that there are two kinds of small-scale bedforms: ribs and step pools, whose the origins of formation have been experimentally examined, have been found to be the type of anti-dunes with coarsening of bed materials and the interaction with diagonal water surface waves (6)(8). The medium-scale bedform was experimentally found to correspond to the alternating bars, which are often observed in alluvial rivers (4). Furthermore, bedforms in which small-scale and medium-scale bedforms coexist have been reproduced in experimental flumes (3). However, the only finding on large-scale bedforms is the one that reveals large-scale bedforms are related to extensively braided streams (5) as well as to the dis-

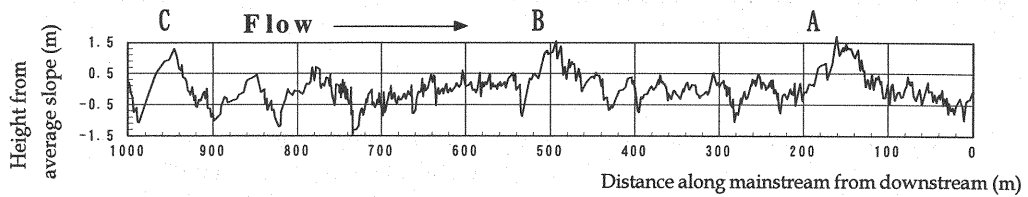


Fig. 1. Longitudinal bed profile in the Shiramizu study section (after the average slope was subtracted).

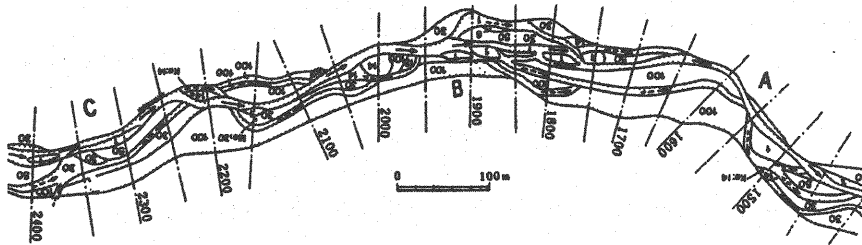
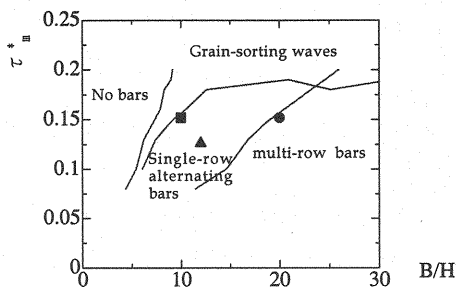
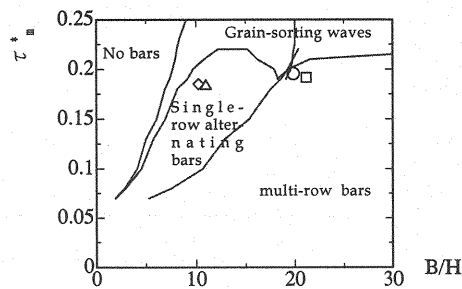


Fig. 2. Plan view in the Shiramizu study section. (A number is partly reverse to make a flow direction correspond.)

covery of sediment discharge from braided streams in Mountain Rivers (1) (2). Therefore, in this study, flume experiments were carried out to reproduce large-scale bedforms by using a steep slope channel and heterogeneous bed materials. Experiments were based on the hypothesis that large-scale bedforms in Mountain Rivers are bed undulations caused by multi-row bars that are formed during times when large floods fill up the whole valley. After these floods, medium- and small-scale bedforms were superposed on the previously formed large-scale bedforms by low water discharge. In this paper, the validity of the hypothesis is examined and the bedforms observed in the experiments are discussed.

#### FIELD INVESTIGATIONS IN SHIRAMIZU RIVER

The Shiramizu River is located in the suburbs of Sapporo in Hokkaido, Japan. It is a typical mountain river with a total length of 8.2 km and a catchment area of 16.46 km<sup>2</sup>. The study site was 1.2 km upstream from the confluence of Usubetsu River. Hasegawa et al. carried out a topological survey of Shiramizu River in 1987 (5). Fig. 1 shows a longitudinal bed profile along the mainstream of Shiramizu River in which the average slope was subtracted. This figure shows that the bed has several undulations with various wavelengths, which can be classified into three different scales: one is the small-scale bedforms, which resemble the shape of teeth. In fact, there are 214 of these bedforms. The mean wavelength of these bedforms is 5.38 m, and the mean wave height is 0.42 m. Another type is the medium-scale bedform with about 1 m step height every 6-10 small-scale bedforms. The wavelengths of this type of bedform range from 30 to 50 m. At the points of 350, 650 and 750 m, relatively small-branched channels were found in the field survey. The third type of bedform is a large-scale bedform which is shown at peaks A, B, C of the undulations in Fig. 1. It should be noted that large-scale bedforms are closely related to the branched channels. These states can be confirmed by comparing Figs. 1 and 2, which are the longitudinal bed profile and the plan view of the same section. The numbers in Fig. 2 indicate the number of years of sediment accumulation, estimated by means of dendrochronology. The solid-line arrows in Fig. 2 show the flow directions of existing channels, and the dotted line arrows illustrate abandoned channels. Figs. 1 and 2 reveal that the branched channels developed from the crests to the troughs of large-scale bedforms, and that they developed in places where the valley width becomes wider from the bottleneck point of the valley. The valley widths of

Fig. 3. Regime criteria for  $I=1/20$ ,  $n=1/4$ Fig. 4. Regime criteria for  $I=1/15$ ,  $n=1/4$ 

the wide parts of Shiramizu River are more than 100 m, and the widths of the narrow parts are about 20 m to 30 m. These data suggest that the formation of large-scale bedforms in Mountain Rivers is closely correlated with the development of branched channels in the valley and with the valley width.

## METHOD AND FLOW CONDITIONS OF EXPERIMENTS

### Method and Instruments

RunL2 series of experiments were performed with a rectangular flume of 20 m in length and 0.6 m in width. Runs L4 and L5 series were performed with a rectangular flume of 10 m in length and 1.2 m in width. These three series of experimental runs were carried out by using the same heterogeneous sediment material. The distribution of grain sizes was coincided with a Talbot distribution defined by equation 1, in which the exponent  $n$  is  $1/4$ .

$$P = (d_i / d_{\max})^n \quad (1)$$

where  $P$  is the weight ratio of bed materials passing through a sieve of  $d_i$ ,  $d_i$  is the grain diameter in the class of the  $i$ -th fraction,  $d_{\max}$  is the maximum grain diameter (1.5 cm), and  $n$  is an exponent. After these materials had been laid in an experimental flume and flattened, an erosive rectangular waterway of 30 cm in width and 2 cm in depth was excavated along the centerline of the flume. Tailgates were installed at the ends of both flumes so that the erosive rectangular waterway could be set up easily. First, a larger water discharge was run along this waterway, and then a lower water discharge was run on the bed which had formed in the larger water discharge. In addition, Runs L2 and L4 series were carried out under no sediment feed conditions, and Run L5 series were carried out under sediment feed conditions.

### Flow Conditions

Figs. 3 and 4 show the regime criteria of linear stability analysis provided by Fujita et al. (3)(7). Based these regime criteria, we determined the flow conditions for the formation of multi-row bars. A summary of the flow conditions is shown in Table 1. From these figures and table, we deduced that multi-row bars formed in the runs with symbols ●, ○ and □, while thought that single-row bars formed in the runs with symbols ■, ▲, △ and ◇. In Table 1,  $Q$  is the water discharge,  $B$  is the channel width,  $t_m^*$  is the Shields shear stress for the mean grain size (0.3 cm),  $H$  is the mean water depth, and  $Fr$  is the Froude number. To determine these values, the Hey equation (Eq.2) (9) was used. It can also be used to estimate the flow resistance for gravel-bed streams, and to conduct experiments on steep channels with heterogeneous bed materials (6)(8).

$$u / u^* = 5.75 \log_{10}(11.16 H / 3.5 d_{84}) \quad (2)$$

Table 1. Experimental conditions.

| Run. | Sign | slope | $Q$<br>(l/s) | $B$<br>(cm) | $B/H$ | $\tau_m^*$ | $Fr$  | Experiment time<br>(minutes) |
|------|------|-------|--------------|-------------|-------|------------|-------|------------------------------|
| L2-0 | ●    | 1/20  | 1.78         | 30          | 20    | 0.152      | 1.037 | 10                           |
| L2-1 | ■    | 1/20  | 0.6          | 15          | 12    | 0.126      | 0.935 | 83                           |
| L2-2 | ▲    | 1/20  | 0.9          | 15          | 10    | 0.152      | 1.037 | 50                           |
| L4-0 | ○    | 1/15  | 2.09         | 30          | 19.9  | 0.203      | 1.201 | 6.5                          |
| L4-1 | □    | 1/15  | 0.843        | 15          | 11.0  | 0.183      | 1.134 | 70                           |
| L4-2 | △    | 1/15  | 1.84         | 30          | 21.2  | 0.191      | 1.161 | 12.5                         |
| L5-0 | ○    | 1/15  | 2.09         | 30          | 19.9  | 0.203      | 1.201 | 6.5                          |
| L5-1 | ○    | 1/15  | 2.09         | 30          | 19.9  | 0.203      | 1.201 | 10.5                         |
| L5-2 | ◇    | 1/15  | 0.87         | 15          | 10.8  | 0.186      | 1.143 | 42.5                         |
| L5-3 | ◇    | 1/15  | 0.88         | 15          | 10.8  | 0.187      | 1.147 | 27.5                         |
| L5-4 | ◇    | 1/15  | 0.87         | 15          | 10.8  | 0.186      | 1.143 | 32.5                         |

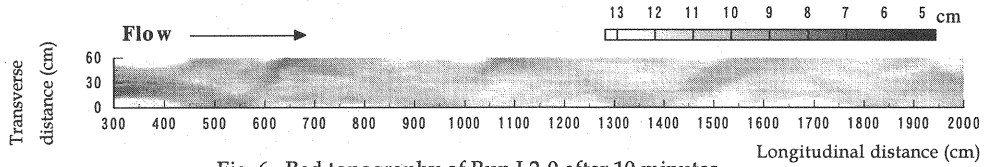


Fig. 6. Bed topography of Run L2-0 after 10 minutes.  
(The average slope was subtracted and height is from the flume bed.)

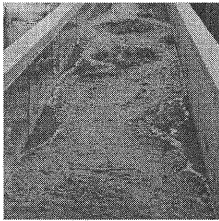


Fig. 5. Photograph of Run L2-0 after 5 minutes.

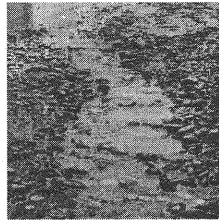


Fig. 7. Photograph of step-pools in Run L2-1 around  $x=1700$  cm.

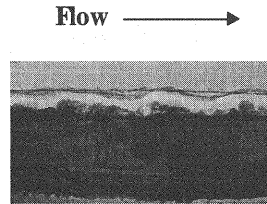


Fig. 8. Photograph of step-pools in Run L2-1 around  $x=1300$  cm.

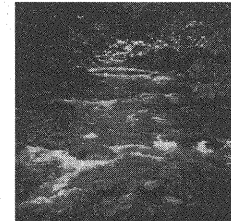


Fig. 9. Photograph of step-pool in Shiramizu River.

where  $u$  is the mean flow velocity,  $u^*$  is the shear velocity, and  $d_{84}$  is the grain diameter finer than 84%.

## RESULTS OF EXPERIMENTS

### Run L2 series Experiments

Run L2-0 was carried out to reproduce multi-row bars and large-scale bedforms. This run was assumed to be a large flood. In our experiment, double-row bars with an average length of about 200 cm formed. About two minutes after starting the water flow, periodic erosion occurred along the sidewall of the waterway, and then a gourd-like pattern formed in the experimental flume. After a few minutes, branched or confluent waterways formed. These configurations formed due to the strong influence of double-row bars as shown in Figs. 5 and 6. Fig. 6 shows the bed topography in Run L2-0 10 minutes after starting the water flow, which is illustrated by the index of the height from the bottom of the flume. The data were obtained at 20 cm intervals in the longitudinal direction and at 1-cm intervals in the transverse direction.

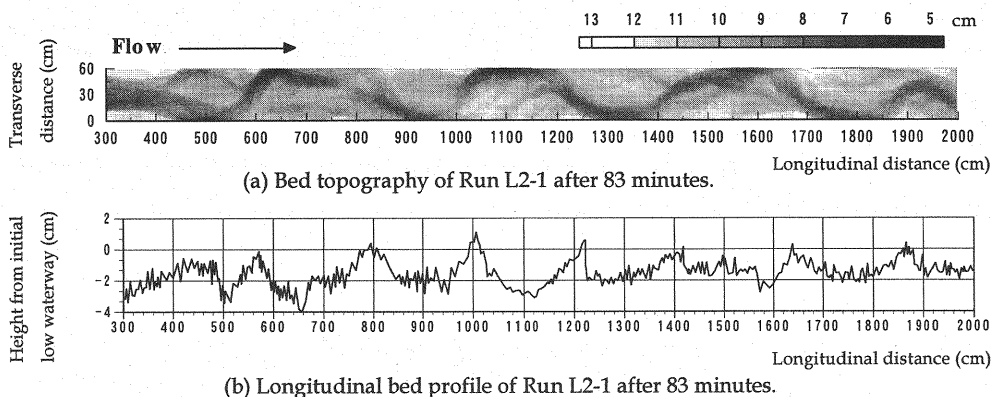


Fig. 10. Bed data of Run L2-2 (a) (b). (The average slope was subtracted.)



Fig. 11. Photograph of Run L2-1 between 1000 cm and 1200 cm.

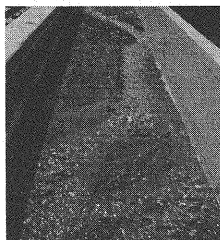


Fig. 12. Photograph of medium scale double row bar in Run L2-1 around 800 cm.

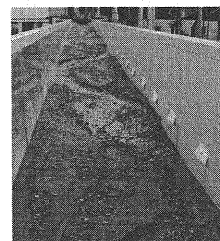


Fig. 13. Photograph of medium-scale bedform after Run L2-2 with a low discharge.

The formation processes of double-row bars in Run L2-0 are similar to the observation made by Ashida, Egashira and Satofuka (1) (2). The formation processes was channel widening, bifurcating and merging.

Run L2-1 was carried out to superpose medium- and small- scale bedforms under the flow conditions in which single-row bars are formed in the each channel (It was estimated that the each channel width was 15 cm because a bifurcated channel formed in Run L2-0). This run was assumed to be a medium or small flood. In this run, small-scale bedforms of transverse ribs and medium-scale bedforms of double-row bars formed on the previously formed bedforms. Figs. 7 and 8 show an overhead view and side view of the formed transverse ribs, respectively. These transverse ribs are very similar to the actual ribs in Shiramizu River as shown in Fig. 9. Fig. 12 shows one of the medium-scale bedforms observed in the waterway. Although they were double-row bars, they were estimated to be equivalent to medium-scale bedforms. This was due to the fact that the wavelengths of the double-row bars were 30 cm to 50 cm, and were much shorter than those of the bedforms which formed in Run L2-0. Fig. 10 (a) shows a topographical contour map of Run L2-1 at 83 minutes after the start of water flow. The data were obtained at intervals of 5 cm in the longitudinal direction and 1 cm in the transverse direction. Fig. 10 (b) shows the longitudinal bed profile along the main stream. The longitudinal bed profile shown in Fig. 10 (b) is very similar to that shown in Fig. 1. This suggests that ups and downs of double-row bars that formed in Run L2-0 are related to those of large-scale bedforms.

Run L2-2 was carried out under approximately the same low flow conditions as those used in Run L2-1. In Run L2-2, both small-scale and medium-scale bedforms were reproduced. A medium-scale bedform formed in the waterway as shown in Fig. 13. In addition, at several bifurcation points, entrances of branched channels became blocked, and therefore the number of waterways decreased. This phenomenon was observed when a large amount of sediment discharge was produced at the

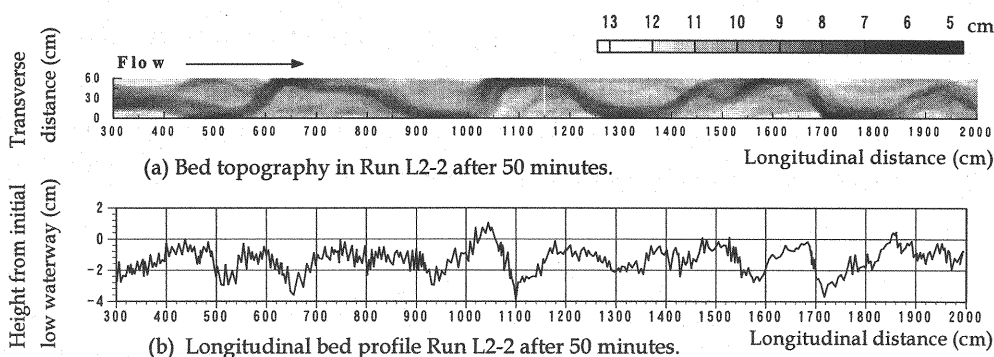


Fig.14. Bed data of Run L2-2 (a) (b) (after the average slope was subtracted.)

upper region of the branching and was deposited rapidly at the entrance of the branched channel. The bed topography and the longitudinal bed profile in Run L2-2 are shown in Figs. 14 (a) and 14 (b), respectively.

The results of Run L2 series demonstrated that three different scales of bedforms found in mountain rivers can be reproduced in an experimental flume, and that a large-scale bedform in a mountain river corresponds to multi-row bars formed by a large flood filling up the valley. Figs. 10(a), 10(b), 14(a) and 14(b) indicate that locations of the bifurcated points correspond to those of the crests of large-scale undulations, and that locations of the apices of channel bends coincide with those of the troughs of large-scale undulations.

#### Run L4 series Experiments

In Run L2 series, it was difficult to clarify the relationship between large-scale bedforms and the valley width as observed in Shiramizu River because the waterway in Run L2 series reached the flume wall soon after the start of water flow. Thus, experiments using a wider experimental flume were conducted (Run L4 series).

Run L4-0 was carried out after the hydraulic condition was determined as multi-row bars formed; multi-row bars and braided channels were observed in this run. A few minutes after starting the test, the initial bed configuration changed due to the presence of slightly irregular multi-row bars with a wavelength of about 2 m in the upper region of the flume. Later, the branched channel along the multi-row bar, as mentioned above, was integrated into the upper region of the flume, and thereafter distinct braided streams appeared in the lower region of the flume. At this time, the beds in the upper region and the lower region tended to become degraded and aggraded, respectively. The bed topography in Run L4 after 6.5 minutes is shown in Fig. 15 (a).

Run L4-1 was carried out after the hydraulic condition was determined as single-row bars formed, which was assumed as a medium or small flood. Small-scale bedforms appeared with a meandering flow. The meandering flow was thought to be equivalent to a medium-scale bedform since its wavelength was about 60 cm. Figs. 15 (b) and 15(c) illustrate the bed topography and the longitudinal bed profile along the mainstream in Run L4-1 at the final stage of the test, respectively. The figures reveal the following: 1) The bed configuration formed in the experiments is a superposition of bedforms of three different scales, similar the one in actual Mountain Rivers. 2) The crest of the large-scale bedform coincides with the starting point of channel branching. In particular, from  $x=600$  cm to 800 cm, several branched channels developed on the steep bed slope toward the trough of the slope. These states are the same as those in Shiramizu River and were also formed in Run L2 series experiments. 3) The entrance of the branched channel was blocked around  $x=450$  cm in Figs. 15 (b) and 16 (a). Fig. 16 shows the cross-sections in Run L4-0 and Run L4-1. From Fig. 16 (a) ( $x=460$  cm), it

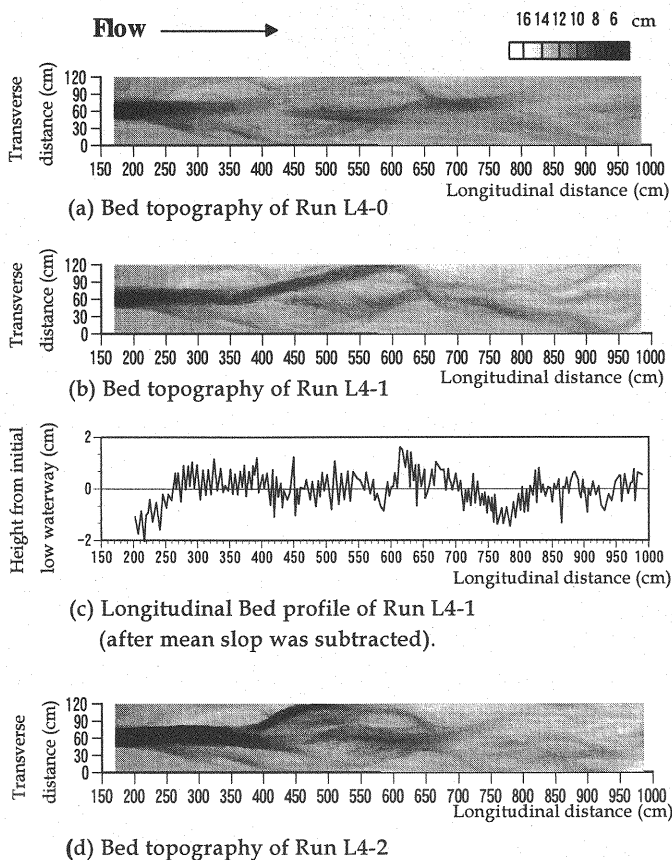


Fig. 15. Bed topographical data of (a) Run L4-0, (b) Run L4-1, (c) Run L4-1, (d) Run L4-2

can be inferred that the old waterway around  $y=60$  cm became blocked and was abandoned. As a result, a new waterway was opened near  $y=90$  cm by the flow in Run L4-1. 4) It should be noted that the confluence point of two waterways at  $x=700$  cm in Run L4-0 shifted to a position in the upper flow region in Run L4-1. As seen in Figs. 15 (b) and 16 (b), the confluence point shifts to  $x=650$  cm, and two waterways of branched channels at  $x=700$  cm appear in Run L4-1. 5) The bed elevation of the waterways of branched channels with small flow discharge is generally high compared with that of the main channel. Figs. 16(c) and (d) show that the bed elevations in the branched waterways (indicated with the arrows in the figures) are higher than those in the mainstream which lie on the left hand of the figures. The differences between the bed elevation of the mainstream and that of the other waterways were also observed in the Shiramizu River, and the difference of the bed elevation is one of the factors that caused blocking at the entrance of a branched channel.

Run L4-2 was carried out under the approximately the same flow conditions as in Run L4-0. A few minutes after starting the run, the blocked entrance of branched channels around  $x=450$  cm opened, and then new double-row bars formed in the re-opened channel. In this run, a remarkable degradation was observed in the upper reach. Thereafter, sediment deposition occurred on the upstream slope of the new formed double-row bar and the angle of bifurcated channels at  $x=350$  cm to  $400$  cm gradually increased. Finally, an entrance block formed on the left side stream which was the mainstream at the beginning. Thus, the mainstream shifted to the right side in the flume. Furthermore, new double-row bars formed in the new mainstream. The bed configuration is shown in Fig.

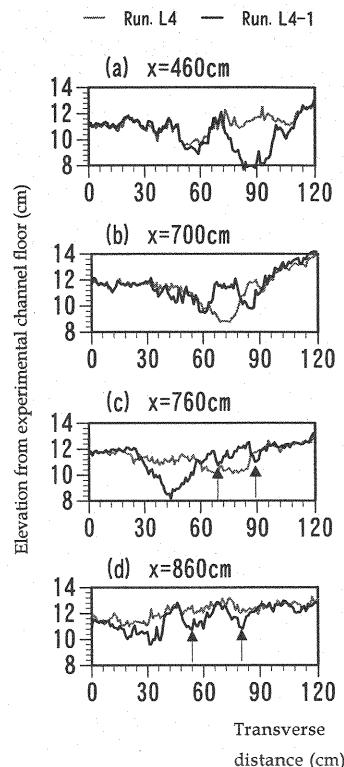


Fig. 16. Cross-sectional change between Run L4-0 and Run L4-1.

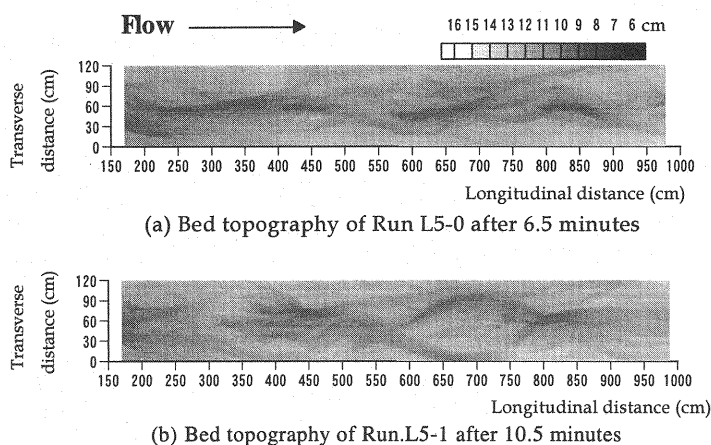


Fig. 17. Bed topographical data of (a) Run L5-0, (b) Run L5-1(After the flume slope was subtracted.)

15 (d), which is the final bed topography in Run L4-2. Fig 15(d) suggests that redevelopment of large-scale bedforms can occur under the conditions of a large amount of flow and sediment transport. The results of Run L4 series revealed that the three superposed bedforms of different scales observed in Run L2 series could also be reproduced in a wider flume. However, the relationship between large-scale bedforms and the valley width that was observed in Shiramizu River could not be clarified. The reason for this is that it was difficult to define the valley width from bed elevation data in the Run L4 series.

#### Run L5 series Experiments

Run L5 series were carried out under sediment feed conditions. These experiments were conducted in order to determine differences between the results under sediment feed conditions and those under no sediment feed conditions. As stated previously, Runs L2 and L4 series were carried out under the no-feed conditions. The total weight and size distribution of sediment feed in Runs L5-0 and L5-1 were determined by referring to the time-averaged sediment discharge in Run L4 experiments, which were measured at the end of the experimental flume. The rate of sediment feed was 119.25 g/s, and the size distribution was slightly finer than that of the initial bed materials. During the experiments, local sediment transport was almost in an equilibrium state because other experimental conditions were the same as Run L4-0, and the amount and the rate of sediment feed were estimated from the observed data in Run L4-0.

The discharge and size distribution of the sediment feed in Runs L5-2, L5-3 and L5-4 were determined from the observed time-averaged sediment discharge at the end of the experimental flume in each run before armoring the streambed. The rate of sediment feed was 18.55 g/s, and the size distribution was much finer than that of the initial bed materials.

Run L5-0 was carried out under the same flow conditions as those in Run L4-0. One minute after starting the run, sidewall erosion occurred and the waterway widened. The waterway around  $x = 400$  cm greatly widened to the left. After three minutes, a bifurcation and a confluence formed in the widened waterway around  $x = 400$  cm and  $x = 700$  cm. Thus, a slightly obscure gourd-like configuration was observed in the whole flume. After that, braided channels were observed in the widened waterway. The bed topography in Run L5-0 6.5 minutes after the start of the experiment is shown in Fig.17 (a).

A comparison of the experimental results of Runs L5-0 and L4-0 at the same time shows that the developing time of the waterway in Run L5-0 was later than that in Run L4-0. It is thought that sedi-

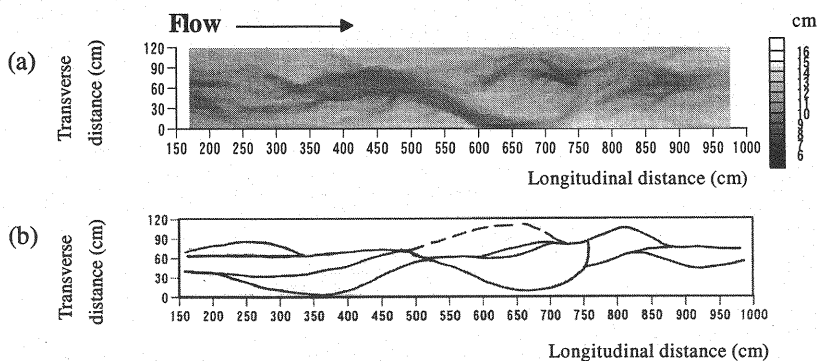


Fig.18. Bed Configuration in Run L5-2 (a) Contor map. (b) Channel pattern.

ment feed conditions may have given rise to local sediment transport equilibrium and delay of bed degradation in the channel.

Run L5-1 was carried out under the same flow conditions as in Run L5-0 because the configuration of multi-row bars was not clear. In this run, a new waterway formed from  $x=550$  cm to  $x=750$  cm two minutes after starting the water flow. Two minutes later, the waterway widened around  $x=300$  cm on the left side of the flume. From six minutes after starting the water flow, braided channels were observed more clearly in the whole area of the flume. Up to eight minutes, a large double-row bar located from  $x=550$  cm to  $x=750$  cm was not submerged. Braided channels and the double-row bars are shown in Fig. 17 (b). This figure shows the bed topography in Run L5-1 at 10.5 minutes after starting the run.

In Run L5-1, the braided channels formed in the upper stream area contrasts with the case in Run L4-0. The configuration and water flow of braided channels in Run L5-1 were similar to those in the lower reach in Run L4-0. This was due to the fact that the sediment feed decreased the channel bed degradation.

Run L5-2 was carried out under approximately the same flow conditions as in Run L4-1. These conditions corresponded to the formation of single-row bars in the waterway (the width of the waterway was estimated 15 cm). At the beginning of this run, water did not flow in the left branched channel around  $x=300$  cm and  $x=500$  cm of the flume because the water discharge decreased approximately by half. However, three branched channels were maintained in the area from  $x=200$  cm to  $x=500$  cm, and two branched channels were maintained in the area from  $x=500$  cm to  $x=750$  cm. After that, the configuration of each braided channel gradually became evident. On the other hand, small-scale bedforms did not form clearly due to the fact that there was less armoring on the surface of each channel, which was caused by the sediment feed from the upstream end of the flume. The final bed topography and channel pattern in Run L5-2 are shown in Figs.18 (a) and 18 (b), respectively.

Run L5-3 was an additional experimental run conducted under the approximately same flow conditions as in Run L5-2. In this run, the closing of existing bifurcated channels and the opening of old bifurcated channels which had formed in Run L5-1, were observed. About ten minutes after starting the run, a bifurcated channel between  $x=200$  cm and  $x=300$  cm closed. This was caused by bed degradation of one channel located in the center of the flume, which caused the flow in the other channel to stop. Thereafter, the closed channel re-opened, which was located from the central flume at  $x=400$  cm to the right flume wall at  $x=700$  cm.

The opening of bifurcated channel in this area was due to water flow concentration and to the overshooting of the flow from the apex of channel bend in a tangential direction. The water flow concentration was caused by the unification of several braided channels in the upper region around

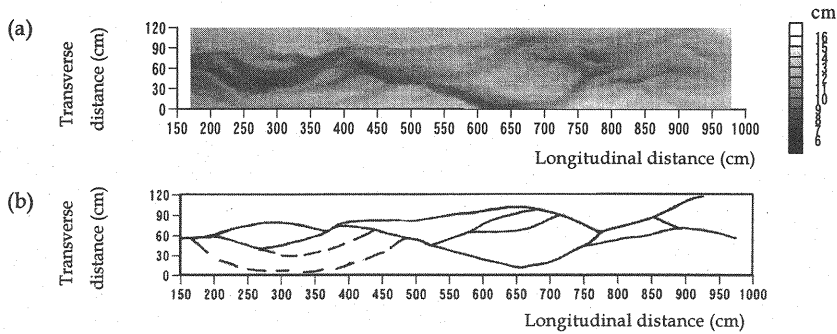


Fig.19. Bed Configuration in Run L5-3 (a) Contor map. (b) Channel pattern.

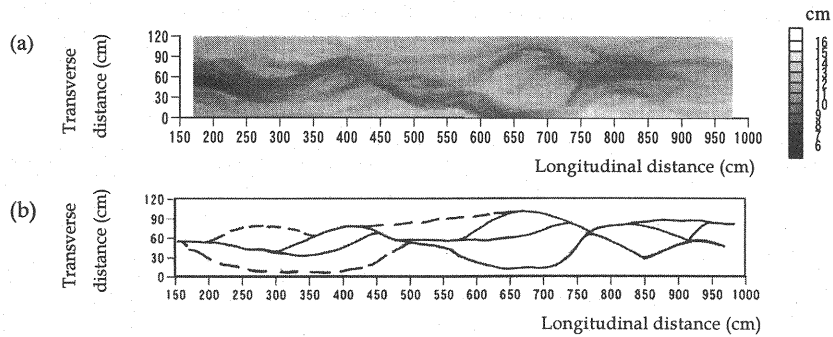


Fig. 20. Bed Configuration in Run L5-4 (a) Contor map. (b) Channel pattern.

$x=400$  cm. The final bed topography and channel pattern in Run L5-3 are shown in Figs.19 (a) and 19 (b), respectively.

Run L5-4 was an additional experimental run conducted under the same flow conditions as in Run L5-3. In this run, the closing of several channels, the opening of an old channel, and the generation of new channels were observed. First, bifurcated channels near  $x = 200$  cm on the left side of the flume closed. This change was caused by a combination of sediment deposition and bed degradation, providing evidence that the following tendencies occurred: 1) sediments began to accumulate at the entrance of a bifurcated channel and 2) water flow became concentrated in the other channel, and then the bed became degraded. As a result, the old channel near  $x = 300$  cm on the right side of the flume opened, and a new channel formed from the top of the curve in water flow near  $x=550$  cm to the position of  $x= 800$  cm. This change was caused by a straightened water flow over the bank near the apex of the channel bend. However, after a period of time, these channels closed, indicating that sediment could be easily deposited in the channels because large amounts of sediment (gravel) were concentrated in the new channel. The final bed topography and channel pattern in Run L5-4 are shown in Figs. 20 (a) and 20 (b), respectively.

Run L5 series experimental results indicated that the size and configuration of double-row bars, that is, those of large-scale bedforms, were very similar in Run L4 and L5 series. Thus, as far as the configuration and size of a large-scale bedform are concerned, sediment feed conditions and no-feed conditions had only a slight influence on the results. The length of large-scale bedforms in Run L5 series experiments was also about 200 cm.

Finally, at the bifurcation from  $x=500$  cm to 800 cm in Run L5-2, L5-3 and L5-4, it was observed that the mainstream changed periodically from the right to the left or in the reverse way within the bifurcated channels. We think that this phenomenon was due to the peculiar blocking and opening mechanisms at the bifurcation point.

Table 2 Mean wavelengths in field investigations and experiments.

|             | Large scal<br>unit(m) | Medium scale<br>unit(m) | Small scale<br>unit(m) | Medium scale/<br>Small scale | Large scale/<br>Medium scale |
|-------------|-----------------------|-------------------------|------------------------|------------------------------|------------------------------|
| Ogawa       | 125.0                 | 34.0                    | 4.2                    | 8.10                         | 3.68                         |
| Shiramizu 1 | 157.0                 | 31.0                    | 5.5                    | 5.64                         | 5.06                         |
| Shiramizu 2 | 400.0                 | 44.0                    | 5.4                    | 8.15                         | 9.09                         |
| Run.L2-2    | 2.272                 | 0.722                   | 0.097                  | 7.424                        | 3.147                        |
| Run.L4-1    | 1.889                 | 0.642                   | 0.082                  | 7.791                        | 2.942                        |

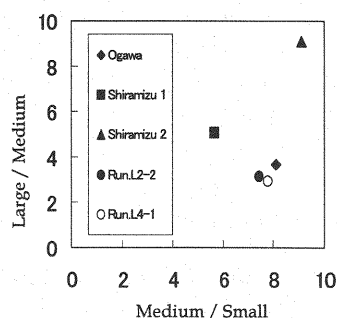


Fig. 21. Comparison of the scale ratios of bedforms of different scales.

### COMPARISON OF THE SCALE RATIOS OF BEDFORMS OF DIFFERENT SCALES

In this section, the mean wavelengths of the bedform of different scales are discussed. The wavelength data discussed here include those from Shiramizu study in section 2 and Shiramizu study section 1 (located downstream of study section 2), Ogawa study section (the river adjacent to Shiramizu River), and Runs L2-2 and L4-1. These data, including mean wavelengths for large-, medium- and small-scale bedforms, and scale ratios for mean wavelengths of the medium- to those of the small-scale bedforms, scale ratios for mean wavelengths of the large- to those of the medium-scale bedforms are shown in Table 2. However, the data from the Run L5 series was not included because the configurations of small-scale and medium-scale bedforms were obscure, and making difficult to measure wavelengths of small- and medium-scale bedforms.

The relationship between the wavelengths of the three kinds of bedform is illustrated in Fig. 21, which show that the horizontal axis is the ratio of medium- to small-scale lengths and the vertical axis is the ratio of large- to medium-scale lengths. The former ratios are grouped around the value of 8, suggesting that there is a correlation between the origin of the formation of small-scale bedforms and that of medium-scale bedforms. On the other hand, the latter ratios are scattered over a wide range of 3 to 9, indicating that the origins of formation of large-scale bedforms and that of medium-scale bedforms are different. Thus, it can be assumed that large-scale bedforms produced various wavelengths due to various runoff discharges of floods in the river. Large floods with a high intensity discharge can cause the formation of bedforms with long wavelengths, while a medium or a small flood can cause the formation of a suitable scale bedform. However, the channel width also affects the wavelength of a generated bedform because the conditions of formation and the mode numbers of multi-row bars are very dependent on the channel width and water depth. The relatively large large-/medium- scale ratio in Shiramizu's study in section 2 may be due to the influence of the valley width (over 100 m), which is greater than the valley width of 20-30 m in the Shiramizu study section 1 or that of 10-30 m in the Ogawa study section. For the same reason, the initial width of an experimental channel affects the wavelength of a bedform. The wavelength in Run L4-1 is a little shorter than that in Run L2-2, though the flume width in Run L4-1 is wider than that in Run L2-2. This is due to the difference in the mode numbers for the generated multi-row bars; the number in Run L4-1 was higher than that in Run L2-2.

### CONCLUSIONS

The following qualitative results were obtained from our experiments:

1. Reproduction of bedforms with three different scales found in mountain rivers can be performed in an experimental flume under different overlapped hydraulic conditions; that is, first a large

water discharge for formation of double-row bars and then a continuous low water discharge on the previously formed bed.

2. It was found that the large-scale bedform in Mountain Rivers correspond to multi-row bars formed by a large floods filling up a valley.
3. The wavelength of a large-scale bedform has a large variety, which is affected by the water discharge rate, the width of the valley, and the initial width of channel.

Although these findings were mainly obtained from experiments under no sediment feed conditions (Run L2 series and Run L4 series), we found that it does not make much difference to the results whether the experiments are performed under sediment no feed conditions or sediment feed conditions (Run L5 series). This means that, as far as configuration and size of bedforms are concerned, sediment feed conditions and no-feed conditions do not produce different results because the size and configuration of double-row bars, that is, those of large-scale bedforms, were very similar in Run L4 series (under no sediment feed conditions) and Run L5 series (under sediment feed conditions). Moreover, several small-scale bedforms and medium-scale bedforms which were approximately the same size as those in Run L2 and Run L4 series were observed in our experiments. However, we found two differences. One difference was that braided channels were developed in the upper area under the sediment feed condition, as can be seen from the results of Runs L5 and L4 series. Another difference was that step-pools were somewhat obscure under sediment feed conditions.

#### REFERENCES

1. Ashida, K., Egashira, S., Satofuka, Y and Gotoh, T. : Variation of Braided Streams and Sediment Discharge, *Annals, Disaster Prevention Research Institute, Kyoto Univ.*, No.33 B-2, pp.241-260, 1990. (In Japanese)
2. Ashida, K., Egashira, S., Satofuka, Y, Gotoh, T and Teranishi, T. : Variation of Braided Streams and Sediment Sorting, *Annals, Disaster Prevention Research Institute, Kyoto Univ.*, No.34 B-2, pp.247-260, 1991. (In Japanese)
3. Fujita, T., Tatsuzawa, H and Hasegawa, K. : Experimental Reproduction and Analyses of Medium-Scale Bedforms in Mountain Rivers, *IAHR Symposium on RIVEER, COASTAL AND ESTUARINE MORPHODYNAMICS*, pp.273-282, 1999.
4. Grant, G.E., Swanson, F.J. and Wolman, M.G. : Pattern and Origin of Stepped-Bed Morphology in High Gradient Streams, *Western Cascades, Oregon, Geological Society of America*, Vol.102, pp.340-352, 1990.
5. Hasegawa, K., Mori, A and Ishikawa, S : Bed Topography and Sediment Transport during Flood in Mountainous Rivers, *Int. Conference on RIVER FLOOD HYDRAULICS* edited by W.R.White, John Wiley and Sons, pp.327-336, 1990.
6. Hasegawa, K. : Hydraulic Characteristics of Mountain Streams and Their Practical Application, *Lecture Notes of the 33rd Summer Seminar on Hydraulic Engineering, Commit. On Hydraulic and Coastal Eng. JSCE*, pp. A-9-1-20, 1997. (in Japanese)
7. Hasegawa, K., Fujita, T. and Meguro, H. : Newly Found Bedforms in Steep Channels with Heterogeneous Bed Materials, *Int. Workshop on River Environments Considering Hydraulic and Hydrologic Phenomena in Snowy and Cold Regions*, pp. 135-143, 2000.
8. Tatsuzawa, H., Hayashi, H and Hasegawa, K. : A Study on Small-scale Bed Topography in Mountain Streams. -Application of step and pool systems for design of a new fish-way, *Journal of Hydraulic, Coastal and Environmental Engineering, JSCE*, vol.656/II, pp.83-103, 2000. (In Japanese)
9. Hey, R.D. : Flow Resistance in Gravel Bed Rivers, *Journal of Hydraulic Division ASCE*, Vol.105, No.4, pp.365-379, 1979.

## APPENDIX - NOTATION

The following symbols are used in this paper:

|            |   |
|------------|---|
| $B$        | = channel width;  |
| $d_i$      | = grain size of bed material in i-th size fraction ;                |
| $d_{\max}$ | = maximum grain size of bed material ;                              |
| $d_{84}$   | = grain size of 84 percentile passing by weight ;                   |
| $Fr$       | = Froude number ;   |
| $H$        | = depth of flow ;   |
| $I$        | = flume slop gradient.  |
| $N$        | = an exponent of the Talbot's distribution ;                        |
| $P$        | = ratio by weight of materials passing a sieve of a size of $d_i$ ; |
| $Q$        | = flow discharge ;  |
| $u$        | = mean flow velocity ;  |
| $u^*$      | = shear velocity; and   |
| $\tau_m^*$ | = Shields shear stress for the mean grain size.                     |

(Received November 12, 2001 ; revised September 10, 2002)